Increasing The Performance Of A 500 W Small Scale Wind Turbine Through Blade Optimization With Low Wind Speed Computational Simulation Studies

Damora Rhakasywi[a, *], Didit Widiyanto[b], Achmad Zuchriadi[c], Bayu Hananto[d], Wildan Amarullah Arrosyid[e]
[a]Mechanical Engineering Department, Faculty of Engineering, Universitas Pembangunan Nasional Veteran Jakarta
Jl. Limo Raya No.80, Limo, Kota Depok, Jawa Barat, 16514, Indonesia
[b]Faculty of Computer Sciences, Universitas Pembangunan Nasional Veteran Jakarta
Jl. RS. Fatmawati Raya, Pd. Labu, Kec. Cilandak, Kota Jakarta Selatan, Daerah Khusus Ibukota Jakarta, 12450, Indonesia
[c] Electrical Engineering Department, Faculty of Engineering, Universitas Pembangunan Nasional Veteran Jakarta
Jl. Limo Raya No.80, Limo, Kota Depok, Jawa Barat, 16514, Indonesia
[d]Faculty of Computer Sciences, Universitas Pembangunan Nasional Veteran Jakarta
Jl. RS. Fatmawati Raya, Pd. Labu, Kec. Cilandak, Kota Jakarta Selatan, Daerah Khusus Ibukota Jakarta, 12450, Indonesia
[e]Mechanical Engineering Department, Faculty of Engineering, Universitas Pembangunan Nasional Veteran Jakarta
Jl. Limo Raya No.80, Limo, Kota Depok, Jawa Barat, 16514, Indonesia
*E-mail: rhakasywi@upnvj.ac.id

Abstract

The world is currently facing a dual energy crisis of increasing energy needs and the negative impact of the use of fossil energy. Indonesia has large wind energy potential, spread across various archipelagic regions. Based on a study by the Ministry of Energy and Natural Resources (ESDM), the potential for wind energy in Indonesia reaches 20,000 GW, with an mean wind speed of 3-7 m/s, proper design of wind turbine blades is an important aspect to ensure optimal performance and energy efficiency under various natural conditions. This research examines the performance and strength of inverse taper type wind turbine blades for horizontal shaft wind turbines, and pays attention to the characteristics of the wind that blows in Indonesia. This research used the method: TSR (tip speed ratio) design, tip to root chord ratio with tip, airfoil variation and determination of two blade segments combine to optimize linear rotation of the reverse tapered blade. Changes are made by going through a shape and performance selection process to determine the best blade using the BEM (blade element momentum) approach. The best designed blade is made from pine wood and its structure is modeled using the finite element method (FEM) to evaluate its safety level when used. The study results show that the best blade produces a peak Cp of 0.486 at a tip speed ratio (TSR) of 5, with a TSR range for Cp above 0.3 reaching 6.444, and can be used at air velocities of up to 15 m/s featuring a factor of safety (FoS) of 1.020.

Keywords: Wind Turbine, Horizontal Shaft, Tip Speed Ratio, Blade Element Momentum, Finite Element Method

Abstrak

Dunia saat ini menghadapi krisis energi ganda kebutuhan energi yang terus meningkat dan dampak buruk dari penggunaan energi fosil. Indonesia memiliki potensi energi angin yang besar, tersebar di berbagai wilayah kepulauannya. Berdasarkan studi Kementerian Energi dan Sumber Daya Alam (ESDM), potensi energi angin di Indonesia mencapai 20.000 GW, dengan kecepatan angin rata-rata 3-7 m/s, perancangan bilah turbin angin yang tepat merupakan aspek penting untuk memastikan kinerja optimal dan efisiensi energi dalam berbagai kondisi alam. Penelitian ini meneliti performa serta kekuatan bilah turbin angin type inverse taper untuk jenis turbin angin poros horizontal, dan memperhatikan karakteristik angin yang berhembus di Indonesia. Penelitian yang dilakukan ini menggunakan metode : TSR (tip speed ratio) rancangan, tip to root chord ratio dengan pangkal, variasi airfoil dan penentuan dua segmen bagian bilah dikombinasikan untuk mengoptimalkan putaran linear pada bilah tirus terbalik. Perubahan dilakukan dengan melalui proses pemilihan bentuk dan kinerja untuk menentukan bilah terbaik menggunakan pendekatan BEM (blade element momentum). Bilah yang dirancang secara paling baik terbuat dari bahan kayu pinus dan strukturnya dimodelkan menggunakan metode elemen hingga (MEH) untuk mengevaluasi tingkat keamanannya saat digunakan. Hasil studi menampilkan bahwa bilah terbaik menghasilkan Cp maksimum sebesar 0,486 pada rasio kecepatan tip (TSR) 5, dengan rentang TSR untuk Cp di atas 0,3 mencapai 6,444, serta dapat digunakan pada kecepatan angin hingga 15 m/s dengan faktor keamanan (FoS) sebesar 1,020.

Kata kunci: Turbin Angin, Poros Horizontal, Tip Speed Ratio, Blade Element Momentum, Metode Elemen Hingga.

1. Introduction

Demand for renewable energy is increasing rapidly in response to climate change issues and the desire to reduce dependence on fossil fuels. Small-scale wind turbines, such as 500 watt wind turbines, are a potential solution for applications in rural areas and households that require an efficient and environmentally friendly energy source. Within the realm of renewable energy, wind stands out as a particularly promising alternative. The development and change of wind energy technology relies heavily on improvements in wind turbines. Various types of wind turbines have been created, many of which are still in the process of development [1]. The study examines a VAWT blade with NACA0015 airfoil using ANSYS FluentTM, validating lift and drag coefficients, adjusting parameters, and comparing thrust predictions [2].

Previous research shows that a higher Reynolds number improves the aerodynamic performance of an airfoil profile, with a higher lift coefficient, lower drag coefficient, and a greater lift to drag ratio. Changes in the Reynolds number affect the optimal shape of the turbine blade, which requires a blunter shape and larger twist angle for maximum efficiency. As a result, turbine blades operating at higher Reynolds numbers have better power coefficients compared to blades at lower Reynolds numbers [3]. Experiments and simulations show 3-blade turbines have the highest power coefficient (2-4% higher) compared to 5 and 6-blade turbines [4]. This study introduces a novel angled winglet design for wind turbines. It enhances power generation by minimizing blade drag and performs effectively on both stationary and mobile platforms [5]. Wind energy is crucial for sustainability. Wind turbines face damage from high-speed winds. A novel solution using aerodynamic control systems, such as chordwise slots on blades, effectively manages turbine speed without hindering power generation [6].

Other studies show that the location of the VAWT affects the performance of the HAWT, with increasing slope having a positive effect and the distance between the VAWT and the HAWT having a negative effect. Taguchi's method shows that placing the two turbines close together with a greater vertical distance produces higher power. The presence of VAWT increases the overall farm output and HAWT output by changing the wind speed vector [7]. Innovative blade profile with fixed trailing-edge flap improves HAWT efficiency by 8.3%, validated via CFD analysis. Annual yield projections favor new design, indicating enhanced performance over reference blade [8]. CFD simulations are used to investigate the effects of coupled platform pitch and surge movements on a floating offshore wind turbine (FOWT). The results show that the coupling of pitch and surge movements at the same frequency and phase causes wind turbine operation to be more unsTable, with large power and thrust fluctuations that can cause fatigue damage to the blades [9]. A low-cost horizontal axis wind turbine designed to reduce energy costs and dependence on non-renewable resources. This research proposes a simpler and more economical alternative to meet the design needs of small scale wind turbines using Polyvinyl Chloride (PVC) as the main material which is simulated using the finite volume method [10]. The study explores wingtip geometric parameters' impact on HAWT performance, using CFD simulations and experimental validation. Lower taper and root chord ratios enhance aerodynamic efficiency, recommending winglets for medium to high wind speed sites [11]. Wind energy is sustainable but turbines face damage from sudden gusts. Aerodynamic braking systems control turbine speed. Proposed method uses along the chord spacing on blades to reduce overspeeding without affecting power generation. Computational analysis optimizes spacing position [12]. In this research, an Actuator Line Method (ALM) was devised to accelerate numerical simulations for urban wind energy applications. Unlike the Actuator Disk Model (ADM), ALM accounts for time-varying blade performance in non-uniform flow conditions, common in urban areas. The study analyzes the NREL Phase VI wind turbine's performance near a tall building at various locations and heights [13].

Floating offshore wind turbines face challenges in severe sea conditions. A control co-design method is proposed for integrated optimization. A framework couples platform hydrodynamics with wind turbines, optimizing platform shape and tuned mass damper. Kriging-enhanced Genetic algorithm is used for efficient optimization. Case study demonstrates significant improvements in power generation and platform stability [14]. Steady computational fluid dynamics with Moving Reference Frame method shows promise for assessing small horizontal-axis wind turbine aerodynamics, but challenges persist in modeling low Reynolds number flows accurately. A comparative literature review reveals inconsistencies in simulation settings, prompting a sensitivity analysis and validation to establish best practices for accurate setups [15]. Wind energy technology is vital due to resource depletion and global warming. This study combines RSM and CFD to optimize ducted wind turbine design. Central Composite Design selects 27 runs. Results show optimal parameters for maximum power output, with potential for sixfold increase. RSM-CFD modeling reduces calculation time and cost [16]. SG6043 Airfoil used in taperless blade design tested with 3, 4, and 5 blades. Simulation shows 3 blades yield highest Cp for low TSR; 3 blades optimal for high TSR [17]. A 5 kW wind turbine blade is optimized using MATLAB and ANSYS. Improved aerodynamics increase power by 7%. Finite Element Method reduces deflections by 42.85%. Blade lifetime ranges from 5.5 to over 20 years [18]. This study investigates the impact of the root-to-hub adapter on HAWT rotor performance, focusing on the transition region between the blade's active part and the hub. Using the NREL Phase VI rotor, a novel CFD-BEM approach was employed, offering reliable results and comprehensive insight into aerodynamic coefficient distribution [19]. Structural integrity analysis involves finite element structural analysis and fluid structural interaction study. Experimental validation helps assess the accuracy of numerical approaches [20]. In this study, HAWT turbine inverse taper blades were used. The types of airfoil used were S1210, S2091, and SD7034. Variations in the design TSR, pitch increase, and the ratio of the tip and base chord lengths of the blade are simulated for the design blade. The blade design is also linearized to improve performance and simplify manufacturing. This research

was carried out in a simulation using TSD-500 wind turbine data as a reference. This research is aimed at obtaining blade variations with the best efficiency and capable of working at low wind speeds.

2. Methodology

This research flow diagram provides a comprehensive overview of the steps taken during the research process. Starting from problem identification, this diagram illustrates each important stage including data collection, analysis, and interpretation of results, to the final conclusion, which is explained in Figure 1.

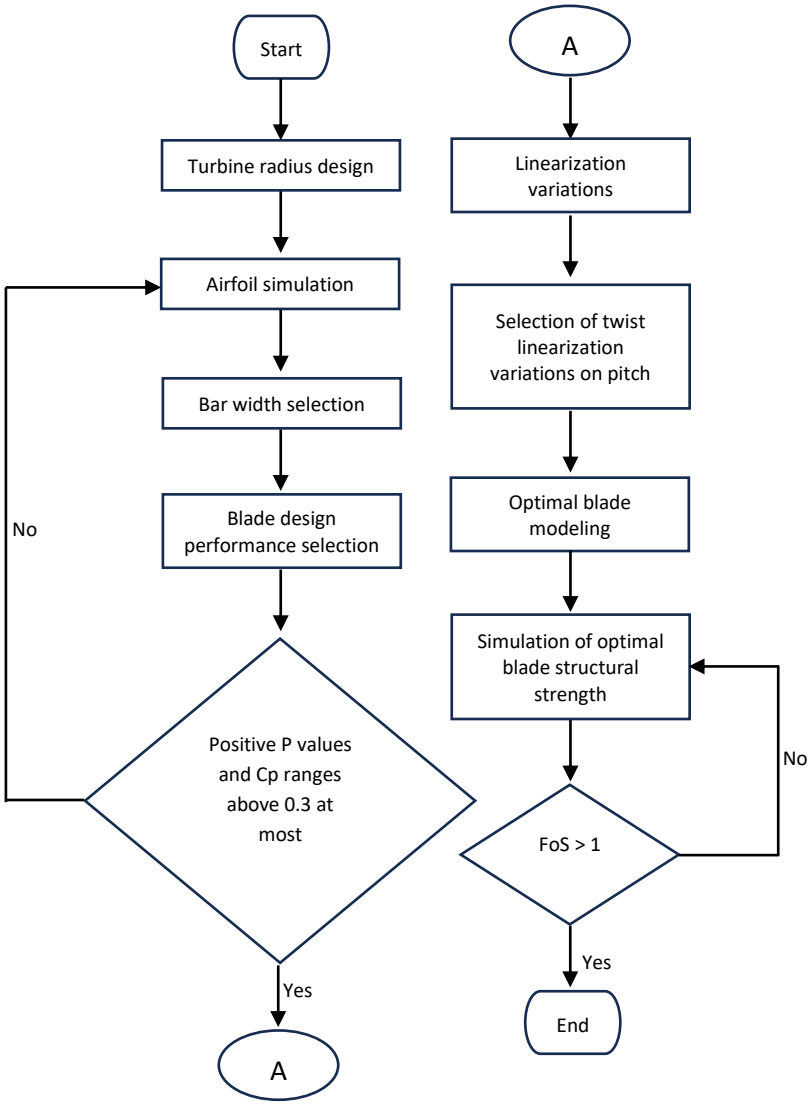

Figure 1. Research flow diagram

2.1 Blade radius design

Blade radius design refers to the process of determining the size and shape of the blades in a machine or device, such as a wind turbine or fan. The radius of the blade is the distance from the center of rotation (hub) to the tip of the blade. Determination of the blade radius describes the turbine efficiency conditions of the system and environmental conditions. Some of the things needed are determined using equations. The power conversion efficiency of a wind turbine system can be determined using a formula [21]:

$$\boldsymbol{K = \eta blade\ X\ \eta transmission\ X\ \eta generator\ X \eta controller}$$

The wind energy absorbed by the blades is determined using the following equation:

$$\boldsymbol{P_{wind} = \frac{P_{rated}}{K}} \quad (1)$$

Blade coverage for each system efficiency with wear:

$$\boldsymbol{P_{wind} = \frac{1}{2}\rho A U^3} \quad (2)$$

The blade radius for the swept area can be calculated by taking the average of the upper and lower limits of blade efficiency thereby finding the required blade radius:

$$\boldsymbol{R} = \sqrt{\frac{\boldsymbol{A}}{\boldsymbol{\pi}}} \quad (3)$$

2.2 Blade radius design

Air flow analysis around the airfoil profile uses a Reynolds number of one million. It is an important study in aerodynamics that helps understand the airflow characteristics, performance and aerodynamic behavior of airfoils under certain conditions.The Reynolds number (Re) is a dimensionless number used in fluid dynamics to predict fluid flow around an object, the ratio of inertial forces to viscous forces in a fluid [22].

$$\boldsymbol{Re} = \frac{\boldsymbol{\rho.V.L}}{\boldsymbol{\mu}} \quad (4)$$

A Reynolds number of one million usually indicates flow that is in the transition range between laminar and turbulent, which often occurs in aerodynamic applications such as aircraft wings and turbine blades. Airfoil evaluation with BEM software uses the assumption of a Reynolds number of one million to compare each airfoil variation with uniform parameters [23]. This simulation uses three types of airfoils S1210 12%, S2091-101-83, and SD7034.

2.3 Determination of the center size of the blade

Determining the blade center size is the process of selecting or determining the width of the hub or blade center on a machine or device that uses a propeller, fan or turbine. The airfoil simulation results obtained are entered into the chord width equation to calculate the approximate chord width at the blade hub to match the dimensions of the TSD-500. The following is a breakdown of the parameters used to calculate the chord width on the hub [24]. The blade chord length is obtained using:

$$\boldsymbol{C} = \frac{\boldsymbol{16\pi R\left(\frac{R}{r}\right)}}{\boldsymbol{9\lambda^2 BC_L}} \quad (5)$$

The flow angle is measured using:

$$\boldsymbol{\varphi} = \frac{\boldsymbol{2}}{\boldsymbol{3}}\boldsymbol{tan^{-1}}\frac{\boldsymbol{1}}{\boldsymbol{\lambda_r}} \quad (6)$$

Twist can be measured using:

$$\boldsymbol{\varphi} = \boldsymbol{\beta} + \boldsymbol{\alpha} \quad (7)$$

2.4 Blade Design Performance Selection

Blade design performance selection is the process of evaluating and selecting the optimal blade design based on various measured and analyzed performance parameters. The blade size selection procedure is carried out by the following method:

1. Ensure the blades produce power at the TSD-500 turbine cut-in speed, 3 m/s which is indicated by a positive value on the P-rpm graph.
2. Displays the Cp-TSR graph in rotor simulation.
3. Design blade dimensions with $Cpmaks$ < 0.3 were sorted because they did not meet the applied lower blade efficiency assumptions.
4. Select the blade with the largest TSR range with a value of $Cp \geq 0.3$

2.5 Optimal Blade Structure Strength Simulation

Optimal blade structural strength simulation is the process of using software and computational techniques to analyze and optimize the strength and structural integrity of blades in various applications, such as wind turbines. This process aims to ensure that the blade can withstand operational and environmental loads without failure or excessive deformation [25][26]. The following is a detailed explanation of this concept:

1. Entering pinus merkusii wood data into the optimal 3D blade model results.
2. Calculate the normal force of the blade with
   $$\boldsymbol{dF_N} = \frac{\boldsymbol{1}}{\boldsymbol{2}}\boldsymbol{\rho U_{rel}^2(C_L cos\varphi + C_D sin\varphi)cdr} \quad (8)$$
3. Get the tangential force value using
   $$\boldsymbol{dF_T} = \frac{\boldsymbol{1}}{\boldsymbol{2}}\boldsymbol{\rho U_{rel}^2(C_L sin\varphi - C_D cos\varphi)cdr} \quad (9)$$
4. Using a fixed support in green, a normal force in purple, and a tangential force in green shown in Figure 2

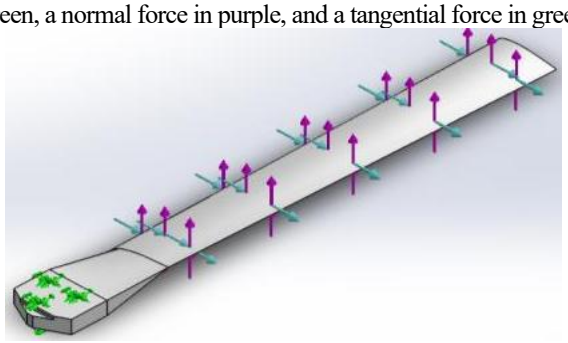

Figure 2. Location of blade loading

5. Make meshing and pay attention to whether the factor of safety is above one ($FoS > 1$) or not in order to know the safety of using the blade.

3. Result and discussion

3.1 Blade radius design results

This research focuses on designing blade radius with the main aim of increasing system efficiency and performance. The design process is carried out through a series of in-depth analyzes and simulations to ensure the resulting blade radius is able to meet predetermined quality and performance standards. The results of this design cover various technical aspects, including efficiency values, wind power, maximum wind speed, blade swept area and blade radius, which are shown in Table 1.

Table 1. Initial Parameters of Wind Turbine Blades

Electric Power Capacity (W)	Efficieny					Wind power (W)	U Max (m/s)	Sweep Area (m^2)	Fingers (m)	Fingers Used
	Blade	Transmission	Generator	Controllers	System					
500	0.30 0.40	0.90	0.90	0.90	0.22 0.29	2286.24 1714.68	12	2.20 1.65	0.84 0.72	**0.78**

Table 1 illustrates the initial parameters of a wind turbine with a power capacity of 500 Watts, including the efficiency of the main components such as the propeller (0.30 and 0.40), transmission, generator, and controller, each of which has an efficiency of 0.90. The total system efficiency is calculated to be 0.22 and 0.29, depending on the configuration. The available wind power is recorded at 2286.24 Watts and 1714.68 Watts, with a maximum wind speed of 12 m/s. The swept area of the propeller varies between 2.20 m² and 1.65 m² according to the tested configuration. In addition, other technical parameters such as the length of the fingers (0.84 m and 0.72 m) and the percentage of finger usage of 0.78 are also analyzed. These data provide an initial insight into the efficiency and performance of the wind turbine system, which can be used as a basis for further evaluation for development and optimization.

The calculation results show that a blade radius of 0.78 m can be used in research because it is located in the middle of the lower and upper limit efficiency of the wind turbine blade, so that the results of the electrical power capacity that will be produced do not experience significant differences in the two blade conditions that may occur.

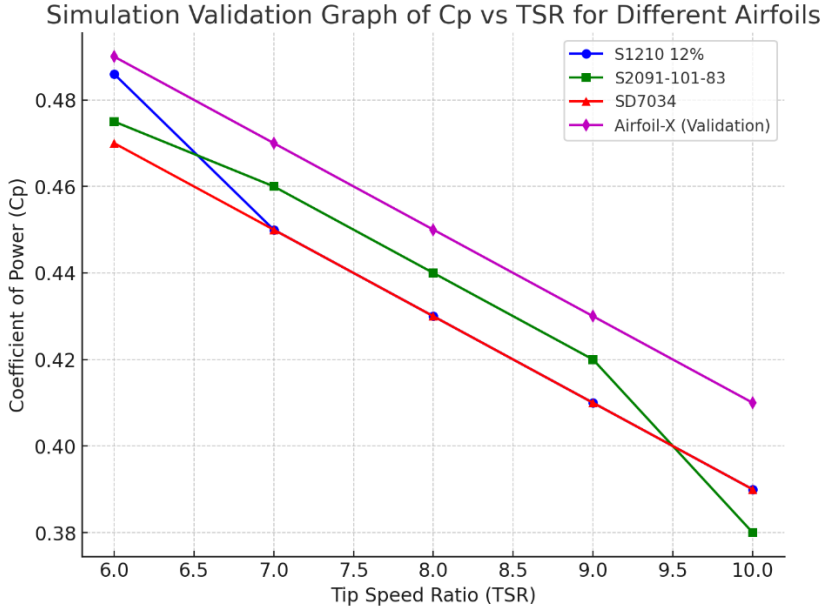

Figure 3. Comparison of Cp vs TSR for Different Airfoils in Wind Turbine Simulation

Figure 3 shows a comparison between the Coefficient of Power (Cp) and Tip Speed Ratio (TSR) for four types of airfoils used in wind turbine simulations. The data in this graph covers three airfoils tested in the study: the S1210 12%, the S2091-101-83, and the SD7034, each of which exhibited different performance over a specific TSR range. These three airfoils were tested at various TSR values to measure the efficiency of the power generated by the wind turbine at varying wind speeds.

An additional line, labeled Airfoil-X (Validation), has been added to the graph as a reference to validate the simulation results. Airfoil-X represents either simulated data that has been validated or experimental data that has already been verified and can be used to compare the wind turbine blade simulations. By including this line, the graph provides a more comprehensive comparison, showing how the simulation results from the tested airfoils align with real-world data or established simulations.

Overall, the graph demonstrates how each airfoil performs at different TSR values, offering insights into the aerodynamic efficiency achievable with different wind turbine blade designs. The inclusion of a validation line boosts confidence in the simulation results, indicating the potential for these designs to be implemented in practical applications, especially in regions like Indonesia, where wind conditions can vary. These findings are crucial for optimizing wind turbine designs, particularly for renewable energy projects in areas with low to moderate wind speeds.

3.2 Airfoil simulation results on a million Reynolds

Aerodynamic parameters in the form of a glide ratio curve to alpha and a CL curve to alpha are sought in this simulation. These two curves function to determine the location of the lift coefficient at the alpha value that can produce the highest airfoil thrust shown in Figure 3 for the three selected types of airfoil. The CL/CD graph helps to understand the aerodynamic efficiency of an airfoil or wing at various angles of attack. Based on pictures (a) and (b), there is the same variable in both curves, namely alpha. Using this curve, start by looking for the largest glide ratio (CL/CD) value, then drag it to the x-axis to find the alpha value. The alpha value that has been found is used to obtain the CL value that will be used. This is due to the uncertainty that the highest CL value in image (b) will be able to produce the largest glide ratio value in image (a). This research requires both curves.

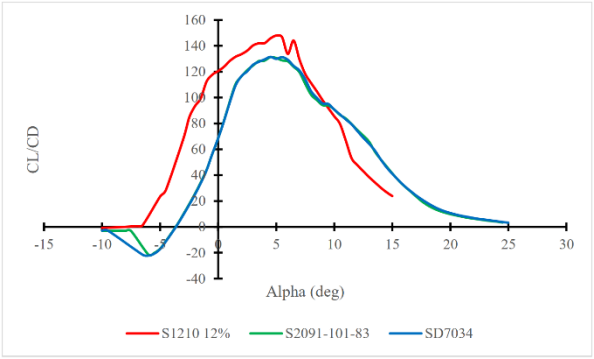

a. CL/CD curve against alpha airfoil for research

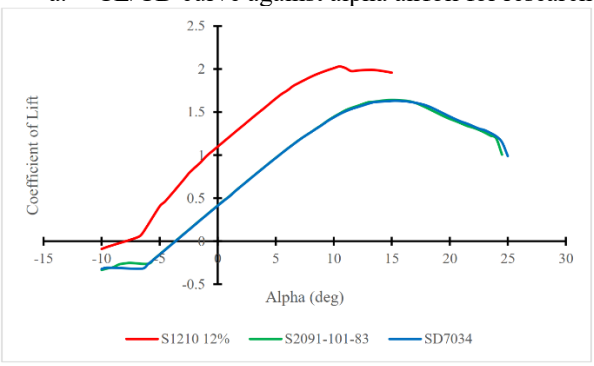

b. CL curve against alpha airfoil against for research

Figure 4. Type of airfoil used in the study

Figure 4 shows the aerodynamic analysis of three types of airfoils: S1210 12%, S2091-101-83, and SD7034. The first graph (a) shows the lift-to-drag ratio (CL/CD) versus angle of attack (Alpha). The S1210 12% airfoil shows the highest CL/CD value at a given angle of attack, indicating better aerodynamic efficiency compared to the other two airfoils, especially at small to medium angles. The SD7034 airfoil has a relatively lower CL/CD performance. The second graph (b) shows the lift coefficient (CL) versus angle of attack. The S1210 12% airfoil reaches a higher maximum CL value than the other airfoils before stalling at large angles of attack. Meanwhile, the S2091-101-83 and SD7034 airfoils have a more stable CL increase but not as high as the S1210 12%. Overall, the S1210 12% airfoil shows the best aerodynamic performance, both in terms of CL/CD efficiency and lift generation capability. This makes it a potential choice for applications requiring high efficiency and maximum lift.

3.3 Blade hub width selection results

Selection of 21 variations of airfoil and TSR combination designs using a TSD-500 type wind turbine. The TSD-500 is a type of wind turbine designed to produce electrical energy from wind with high efficiency and performance. The TSD-500 wind turbine is an efficient and sustainable energy solution to meet modern energy needs.

Table 2. Innermost station width

Variations in design parameters	S1210 12%						
	TSR 4	TSR 5	TSR 6	TSR 7	TSR 8	TSR 9	TSR 10
Root chord length (c)	0.253	0.162	0.112	0.082	0.063	0.050	0.040
Base twist (deg)	27.62	23.37	19.95	17.17	14.90	13.02	11.44
Innermost station width (z)	0.285	0.176	0.119	0.086	0.065	0.051	0.041
Selection 0.080 ≤ innermost station width ≤ 0.155	Not pass	Not pass	Passed	Passed	Not pass	Not pass	Not pass
Variations in design parameters	S2091-101-83						
	TSR 4	TSR 5	TSR 6	TSR 7	TSR 8	TSR 9	TSR 10
Root chord length (c)	0.458	0.293	0.204	0.217	0.115	0.090	0.093
Base twist (deg)	28.12	23.87	20.45	17.67	15.40	13.52	11.94
Innermost station width (z)	0.519	0.321	0.217	0.157	0.119	0.093	0.075
Selection 0.080 ≤ innermost station width ≤ 0.155	Not pass	Not pass	Not pass	Not pass	Passed	Passed	Not pass
Variations in design parameters	SD7034						
	TSR 4	TSR 5	TSR 6	TSR 7	TSR 8	TSR 9	TSR 10
Root chord length (c)	0.458	0.293	0.204	0.150	0.115	0.090	0.073
Base twist (deg)	28.12	23.87	20.45	17.67	15.40	13.52	11.94
Innermost station width (z)	0.519	0.321	0.217	0.157	0.119	0.093	0.075
Selection 0.080 ≤ innermost station width ≤ 0.155	Not pass	Not pass	Not pass	Not pass	Passed	Passed	Not pass

Table 2 shows the chord width of the turbine blade at the point closest to the hub or center of rotation of the turbine. The width of the innermost station on a wind turbine blade has several important functions related to the aerodynamic and structural performance of the turbine. Table 2 evaluates the wind turbine blade design parameters based on the variation of Tip Speed Ratio (TSR) values for three blade profiles: S1210 12%, S209-101-83, and SD7034. The parameters analyzed include root chord length, base twist angle, and deepest station width, with design criteria. For the S1210 12% profile, only TSRs 6 and 7 meet the design criteria, while the other TSRs do not pass. Profiles S209-101-83 and SD7034 show similar results, with the deepest station width meeting the criteria for TSRs 7, 8, and 9, but not for the other TSRs. These results indicate that not all combinations of profiles and TSR values meet the design criteria, so parameter optimization is needed to achieve the desired performance.

3.5 Blade design performance selection results

The blade design performance selection method serves to ensure the suitability of the blade with the low cut-in speed of the TSD-500 turbine and can select the best blade based on the resulting performance. Cut-in speed is the minimum wind speed at which a wind turbine starts producing electricity. At wind speeds below the cut-in speed, the wind turbine will not produce enough electrical power to be distributed to the electricity grid for use, which is explained in Tables 3, 4 and 5.

Table 3. S1210 Blade power 12% to rotational speed at wind speed 3 m/s

Omega (rpm)	TSR 6 R 1,10 P (W)	TSR 6 R 1,20 P (W)	TSR 6 R 1,30 P (W)	TSR 7 R 1,10 P (W)	TSR 7 R 1,20 P (W)	TSR 7 R 1,30 P (W)
1	0.0562805	0.0590689	0.061788	0.037465	0.040272	0.0417489
101	12.5572	12.3614	12.2086	10.1851	10.9323	10.9102
201	5.07551	4.02838	2.69414	7.53913	6.9801	5.89884
301	-13.8334	-15.9971	-19.8925	-9.80385	-10.8436	-13.6297
401	-58.0544	-58.0973	-69.4342	-40.5835	-44.0621	-47.8027
501	-115.185	-126.05	-130.091	-96.8813	-94.809	-115.743
601	-217.637	-235.157	-255.982	-175.621	-179.773	-201.73
701	-355.78	-397.698	-442.914	-281.505	-285.805	-362.803
801	-566.262	-644.294	-674.542	-425.121	-481.08	-524.712
901	-887.275	-926.972	-996.639	-647.819	-660.667	-777.344
1001	-1247.61	-1297.24	-1371.25	-946.28	-880.686	-1081.7

Table 3 shows the blade power of the S1210 12% profile at various rotational speeds (omega), wind speed of 3 m/s, and TSR combinations (6 and 7) with blade radii of 1.10 m, 1.20 m, and 1.30 m. At low rotational speed (1 rpm), the initial power is positive for all configurations, indicating that energy is being generated. However, as the rotational speed increases, the power starts to become negative, reflecting the increasing aerodynamic loads that cause energy losses. The negative power is first seen at a rotational speed of 301 rpm for TSR 6, radius 1.10 m, and continues to decrease drastically at higher speeds in all configurations. This indicates that there is an optimal limit to the rotational speed to maximize the efficiency of the wind turbine system. This trend emphasizes the importance of designing and regulating the rotational speed to reduce power losses and improve wind turbine performance.

Table 4. S2091-101-83 Blade power to rotational speed at wind speed 3 m/s

Omega (rpm)	TSR 8 R 1,10 P (W)	TSR 8 R 1,20 P (W)	TSR 8 R 1,30 P (W)	TSR 9 R 1,10 P (W)	TSR 9 R 1,20 P (W)	TSR 9 R 1,30 P (W)
1	0.026559	0.028301	0.0311839	0.019657	0.0207717	0.0218126
101	10.258	10.815	11.068	7.80096	8.70635	9.0976
201	10.8845	10.5363	10.8575	11.8593	11.3988	11.0146
301	3.31311	2.54067	3.40816	5.21601	4.28012	3.524
401	-10.6659	-12.0238	-10.0098	-6.75137	-8.75782	-10.118
501	-32.0363	-34.0413	-30.1025	-26.2865	-29.4976	-31.4491
601	-62.085	-65.3162	-58.724	-53.8941	-58.8655	-61.4059
701	-102.008	-106.437	-96.6028	-90.9655	-98.1048	-101.268
801	-160.782	-159.836	-172.183	-139.021	-148.468	-153.189
901	-243.424	-254.764	-248.452	-199.245	-212.553	-218.103
1001	-335.396	-350.381	-337.968	-272.329	-293.832	-300.909

Table 4 shows the blade power of the S2091-101-83 profile at rotational speeds (omega), TSR (Tip Speed Ratio) 8 and 9, and radii of 1.10 m, 1.20 m, and 1.30 m, with a constant wind speed of 3 m/s. At low rotational speeds (omega = 1 rpm), the initial power is positive indicating that energy is generated. However, the power begins to decrease and becomes negative at TSR 8 and 9. This power decrease is greater at high rotational speeds, with the highest negative value at TSR 8 with a radius of 1.10 m (-335.396 W). These results indicate that too high a rotational speed increases the aerodynamic load and causes energy loss. Therefore, it is important to determine the optimal rotational speed so that the efficiency of the wind turbine system can be maximized.

Table 5. SD7034 Blade power to rotational speed at wind speed 3 m/s

Omega (rpm)	TSR 8 R 1,10 P (W)	TSR 8 R 1,20 P (W)	TSR 8 R 1,30 P (W)	TSR 9 R 1,10 P (W)	TSR 9 R 1,20 P (W)	TSR 9 R 1,30 P (W)
1	0.0264789	0.0280472	0.0290181	0.0194512	0.02029	0.0214804
101	10.6699	10.8613	10.7701	7.99506	8.61584	9.10044
201	10.9267	10.5017	9.78664	11.7582	11.2779	10.8227
301	3.50298	2.55994	0.926096	5.10377	3.85257	3.20014
401	-10.1714	-11.9263	-14.847	-6.73898	-9.28519	-10.6136
501	-30.8637	-33.8093	-39.151	-26.0923	-30.3838	-32.348
601	-60.6341	-65.1414	-73.0946	-53.8022	-60.4106	-63.1414
701	-100.401	-106.812	-118.668	-90.9152	-100.557	-104.295
801	-151.623	-161.708	-183.531	-139.102	-152.624	-157.622
901	-237.022	-251.035	-273.369	-199.04	-217.627	-224.456
1001	-328.719	-339.662	-374.396	-273.429	-297.932	-306.016

Table 5 shows the blade power of SD7034 profile at rotational speed (omega), TSR (Tip Speed Ratio) 8 and 9, and radius of 1.10 m, 1.20 m, and 1.30 m with a constant wind speed of 3 m/s. At low rotational speed (omega = 1 rpm), the initial power is positive, indicating the energy produced by the propeller. However, the power starts to decrease and becomes negative at increasing energy losses due to aerodynamic loads. At TSR 8, the largest negative power was recorded for a radius of 1.10 m. A similar trend is seen in TSR 9, where the negative power increases at larger radii, such as for a radius of 1.30 m at the same rotational speed. These results emphasize the importance of optimal rotational speed settings to minimize power losses and maximize the operational efficiency of wind turbines.

Cp (coefficient of power) and TSR (Tip Speed Ratio) are two important parameters in assessing wind turbine performance. Cp is the ratio between the power produced by the wind turbine and the total power available in the wind hitting the rotor. Cp functions to determine the efficiency value of the wind turbine for converting wind energy into mechanical energy which is explained in Table 6.

Table 6. CP Range to Blade TSR

Variation of Design Parameters	S1210 12%					
	TSR 6 R 1,10	**TSR 6 R 1,20**	**TSR 6 R 1,30**	**TSR 7 R 1,10**	**TSR 7 R 1,20**	**TSR 7 R 1,30**
TSR range at Cp >= 0.3	2.270 - 4.502	2.234-4.316	2.197-4.113	2.648-5.045	2.559-4.907	2.554-4.684
Difference	2.232	2.082	1.916	2.397	2.348	2.13
Variation of Design Parameters	**S2091-101-83**					
	TSR 8 R 1,10	**TSR 8 R 1,20**	**TSR 8 R 1,30**	**TSR 9 R 1,10**	**TSR 9 R 1,20**	**TSR 9 R 1,30**
TSR range at Cp >= 0.3	2.670-6.191	2.514-6.028	2.428-6.211	2.929-6.714	2.878-6.464	2.818-6.272
Difference	3.521	3.514	3.783	**3.785**	3.586	3.454
Variation of Design Parameters	**SD7034**					
	TSR 8 R 1,10	**TSR 8 R 1,20**	**TSR 8 R 1,30**	**TSR 9 R 1,10**	**TSR 9 R 1,20**	**TSR 9 R 1,30**
TSR range at Cp >= 0.3	2.603-6.214	2.507-6.017	2.457-5.672	2.921-6.687	2.849-6.372	2.829-6.303
Difference	3.611	3.51	3.215	3.766	3.523	3.474

Table 6 shows the Tip Speed Ratio (TSR) range at power coefficient (Cp) ≥ 0.3 for three propeller profiles: S1210 12%, S2091-101-83, and SD7034. The TSR range is calculated as the difference between the upper and lower limits of TSR for each radius (R) configuration. In the S1210 12% profile, the largest TSR range is found in the TSR 7 R 1.20 configuration with a difference of 2.348. The S2091-101-83 and SD7034 profiles show a wider TSR range than the S1210 12%. The largest range in S2091-101-83 is 3.783 (TSR 8 R 1.30), while in SD7034 it is 3.766 (TSR 8 R 1.20). These

results show that the S2091-101-83 and SD7034 profiles are more optimal in maintaining power efficiency at various TSR values, making them more suitable for applications with high performance requirements.

3.5 Selection results of twist linearization variations

Varying twist linearization requires a selection process to choose the angle that best suits the research design blade. The results of the twist angle geometry selection resulted in 46 variations that passed. Variations that pass will be simulated to determine their performance using airfoil blade dimensions S2091-101-83 with a TSR 9 and a base to tip ratio of 1,10. Linearization of blade twist in wind turbine design is the process of adjusting the blade angle along the length of the blade linearly to optimize aerodynamic performance and turbine efficiency values, which are explained in Table 7. Linearization of twist in wind turbine blades is a design technique that optimizes the blade angle from base to tip in a linear manner to increase aerodynamic efficiency and structural strength. Each part of the blade operates at an optimal angle of attack, twist linearization helps increase the power coefficient (Cp) and more even load distribution, reducing stress and vibration which can extend blade life and reduce maintenance costs. This method simplifies the design and production process, as consistent angle changes make it easier to use simulation software and reduce manufacturing complexity. The implementation of twist linearization allows the wind turbine to operate efficiently over a wide range of wind speeds, ensuring optimal performance across a wide range of operational conditions. Research and case studies demonstrate the importance of this approach in achieving maximum energy efficiency and increasing wind turbine reliability.

Table 7. Research blade twist linearization performance selection

Variation of Design Parameters	TSR range at Cp >= 0.3		Difference	Variation of Design Parameters	TSR range at Cp >= 0.3		Difference
Initial Design		2.929-6.714	3.785		Linear 2 & 8	2.741-8.260	5.519
Twist + Pitch 0 deg	Linear 6 & 8	2.959-6.555	3.596		Linear 2 & 9	2.745-8.221	5.476
	Linear 0 & 10	2.690-8.520	5.83		Linear 2 & 10	2.728-8.417	5.689
	Linear 1 & 10	2.757-8.086	5.329		Linear 3 & 4	2.805-7.710	4.905
	Linear 2 & 10	2.796-7.818	5.022		Linear 3 & 8	2.751-8.165	5.414
	Linear 3 & 8	2.831-7.544	4.713		Linear 3 & 9	2.762-8.056	5.294
	Linear 3 & 10	2.832-7.548	4.716		Linear 3 & 10	2.751-8.166	5.415
	Linear 4 & 8	2.839-7.526	4.687		Linear 4 & 8	2.753-8.136	5.383
	Linear 4 & 10	2.841-7.495	4.654		Linear 4 & 9	2.780-8.021	5.241
	Linear 5 & 8	2.850-7.450	4.6	Twist + pitch 2 deg	Linear 4 & 10	2.755-8.112	5.357
	Linear 5 & 9	2.863-7.266	4.403		Linear 5 & 8	2.778-8.070	5.292
	Linear 5 & 10	2.858-7.338	4.48		Linear 5 & 9	2.788-7.936	5.148
	Linear 6 & 8	2.873-7.199	4.326		Linear 5 & 10	2.784-7.990	5.206
	Linear 6 & 9	2.889-7.008	4.119		Linear 6 & 7	2.845-7.454	4.609
	Linear 6 & 10	2.889-7.008	4.119		Linear 6 & 8	2.823-7.805	4.982
	Linear 7 & 9	2.899-6.836	3.937		Linear 6 & 9	2.833-7.660	4.827
	Linear 7 & 10	2.898-6.833	3.935		Linear 6 & 10	2.833-7.657	4.824
	Linear 8 & 10	2.832-7.544	4.712		Linear 7 & 8	2.848-7.469	4.621
	Linear 9 & 10	2.889-7.017	4.128		Linear 7 & 9	2.850-7.508	4.658
	Linear 0 & 9	2.677-8.659	5.982		Linear 7 & 10	2.849-7.508	4.659
	Linear 0 & 10	**2.643-9.087**	**6.444**		Linear 8 & 9	2.738-8.299	5.561
Twist + Pitch 2 deg	Linear 1 & 8	2.731-8.354	5.623		Linear 8 & 10	2.751-8.163	5.412
	Linear 1 & 9	2.717-8.399	5.682		Linear 9 & 10	2.832-7.671	4.839
	Linear 1 & 10	2.693-8.652	5.959				

The length of the TSR range in table 7, from research shows that the designed blade has the best performance on linear twist elements 0 and 10 with a pitch increase of 2 degrees. Table 7 shows the effect of variations in the blade design parameters, especially the blade twist linearization and pitch angle (0° and 2°), on the range of Tip Speed Ratio (TSR) values with a power coefficient (Cp) ≥ 0.3. In the initial design, the TSR range is 2.929–6.714 with a difference of 3.785. Several combinations of linearity and pitch show improved performance, with a pitch angle variation of 2° producing a wider TSR range than a pitch of 0°. The best combination is found in linear 0 & 10 with a pitch angle of 2°, producing a TSR range of 2.643–9.087 and a difference of 6.444, which is a significant improvement compared to the initial design. These results indicate that adjusting the twist linearity and pitch angle can improve the efficiency and flexibility of wind turbine blades under various operating conditions.

3.6 Wind turbine blade design and structural strength

Optimal blade modeling results show that designs with linear twist provide even load distribution and optimal angles of attack at each blade section, improving aerodynamic efficiency and energy performance. In addition, the optimal blade structural strength simulation results confirm that this design not only improves the energy performance but also strengthens the structural durability of the blade, reducing the risk of damage and extending the operational life of the wind turbine. The combination of aerodynamic modeling and structural strength simulation ensures that wind turbine blades can operate efficiently and reliably under a wide range of wind speed conditions. The design of blade dimensions

at this stage uses S2091-101-83 airfoil with TSR 9, base to tip length ratio of 1.10, linear element twist of 0 & 10, and pitch increment of 2 degrees.

The normal force equation dFN is used to calculate the aerodynamic force perpendicular to the blade due to the interaction of fluid flow. This force is calculated based on parameters such as fluid density (ρ), relative flow velocity (Urel), lift coefficient (CL), drag coefficient (CD), relative flow angle (ϕ), blade chord length (c), and radial blade length element (dr) written in equations 9 and 10. The results of this calculation are important for analyzing the structural loads experienced by the blade. The tangential force equation calculates the force parallel to the blade rotation axis. This tangential force plays a role in calculating the rotational moment and power generated by the blade. This equation uses the same parameters as, but focuses on the force components that are directly related to rotational performance and power efficiency. These two equations are very important in the simulation of optimal blade structures, such as in wind turbines or propulsion blades. By calculating the distribution of normal and tangential forces along the blade, the design can be optimized to efficiently resist aerodynamic loads, increase structural strength, and maximize aerodynamic performance.

Factor of Safety (FoS) is a measure used in engineering and engineering design to ensure that a structure or component has sufficient strength to withstand the expected load plus an additional safety margin. FoS is the ratio between the maximum capacity that a structure or component can withstand and the maximum load that is expected to occur during its use. The Factor of Safety (FoS) value for wind speed obtained from the blade structure strength simulation results is shown in Figure 4

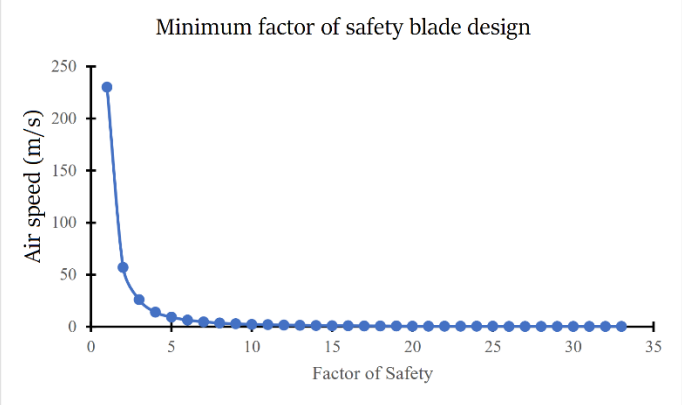

Figure 4. Optimal blade safety factor for wind speed

The simulation results shown in Figure 4 explain that a wind speed of 15 m/s is the safety limit for using the optimal blade design in this research, with an FoS value of 1.020. The following picture explains the factor of safety at a wind speed of 15 m/s.

Figure 4 shows the relationship between wind speed (air speed) in meters per second (m/s) and the factor of safety in the design of wind turbine blades. This graph aims to identify the minimum value of the safety factor required at various wind speeds to ensure operational stability and safety. From the graph, it can be seen that at high wind speeds, such as above 200 m/s, the value of the factor of safety is quite low (approaching 1). However, when the wind speed decreases below 50 m/s, the factor of safety increases significantly until it reaches a constant value after about 5. This graph reflects the importance of adjusting the design of the blades at low wind speeds to achieve an optimal level of safety, while at high speeds, the design tends to focus more on structural strength because the safety factor is relatively low.

4. Conclusions

This article provides adequate answers to the problems and research objectives that have been set, with a focus on the design of inverse taper type wind turbine blades. This study uses the Blade Element Momentum (BEM) and Finite Element Method (FEM) methods to analyze the performance and strength of the blades, aiming to optimize the blade design so that it can function efficiently in varying wind conditions, especially in Indonesia which has great wind energy potential. The final results presented show that the designed blade produces a maximum peak power coefficient (Cp) of 0.486 at a tip speed ratio (TSR) of 5, with the TSR range for Cp above 0.3 reaching 6.444. These findings are logical and supported by data obtained from simulations and analyses conducted, providing confidence in the validity of the research results. The implications of this study are significant, especially in the context of renewable energy development in Indonesia, where optimal wind turbine blade design can improve the efficiency and competitiveness of wind energy as an alternative energy source. This study also provides new insights into how blade design can be tailored to improve performance under different wind conditions, which is highly relevant for practical applications in the field. In addition, this paper recommends several suggestions for further research, including further exploration of airfoil profile variations and pitch angle adjustments to improve blade efficiency. Further research is also needed to explore the impact of blade design variations on turbine performance under extreme wind conditions, which is important to ensure that the proposed design is not only efficient but also durable and safe in the long term. Overall, this article makes a significant contribution to the understanding and development of wind turbine blade design, comprehensively answers the research questions and

presents logical results, and paves the way for further research that can improve the efficiency and sustainability of wind energy. Thus, the results of this study are expected to be useful in the development of renewable energy technologies in the future.

Acknowledgement

This work was supported within the LPPM – Universitas Pembangunan Nasional Veteran Jakarta (Project number: 1044/UN61.0/HK.02/2022). The author would like to thank the renewable energy research team for assisting in providing research equipment.

Daftar Pustaka

[1] R. A. Kishore and S. Priya, "Design and experimental verification of a high efficiency small wind energy portable turbine (SWEPT)," *J. Wind Eng. Ind. Aerodyn. J.*, vol. 118, pp. 12–19, 2013, doi: 10.1016/j.jweia.2013.04.009.

[2] C.-J. Bai, Y.-Y. Lin, S.-Y. Lin, and W.-C. Wang, "Computational fluid dynamics analysis of the vertical axis wind turbine blade with tubercle leading edge," *J. Renew. Sustain. Energy*, vol. 7, no. 3, pp. 1–14, 2015, doi: 10.1063/1.4922192.

[3] M. Ge, D. Tian, and Y. Deng, "Reynolds Number Effect on the Optimization of a Wind Turbine Blade for Maximum Aerodynamic Efficiency," *J. Energy Eng.*, vol. 142, no. 1, pp. 1–12, 2014, doi: 10.1061/(ASCE)EY.1943-7897.

[4] A. Eltayesh *et al.*, "Experimental and numerical investigation of the effect of blade number on the aerodynamic performance of a small-scale horizontal axis wind turbine," *Alexandria Eng. J.*, vol. 60, no. 4, pp. 3931–3944, 2021, doi: 10.1016/j.aej.2021.02.048.

[5] Z. Zhang *et al.*, "Comparative analysis of bent and basic winglets on performance improvement of horizontal axis wind turbines," *Energy*, vol. 281, no. July, p. 128252, 2023, doi: 10.1016/j.energy.2023.128252.

[6] B. N. Kumar, K. M. Parammasivam, P. N. S. C, and R. A. C, "Feasibility analysis of novel aerodynamic braking system for horizontal axis wind turbines," *Mater. Today Proc.*, vol. 68, no. xxxx, pp. 1–7, 2022, doi: 10.1016/j.matpr.2022.06.444.

[7] C. Pichandi, P. Pitchandi, S. Kumar, and N. M. Sudharsan, "Improving the performance of a combined horizontal and vertical axis wind turbine for a specific terrain using CFD," *Mater. Today Proc.*, vol. 62, pp. 1089–1097, 2022, doi: 10.1016/j.matpr.2022.04.317.

[8] A. Mansi and D. Aydin, "The impact of trailing edge flap on the aerodynamic performance of small-scale horizontal axis wind turbine," *Energy Convers. Manag.*, vol. 256, no. December 2021, pp. 1–18, 2022, doi: 10.1016/j.enconman.2022.115396.

[9] Y. Guo, X. Wang, Y. Mei, Z. Ye, and X. Guo, "Effect of coupled platform pitch-surge motions on the aerodynamic characters of a horizontal floating offshore wind turbine," *Renew. Energy*, vol. 196, pp. 278–297, 2022, doi: 10.1016/j.renene.2022.06.108.

[10] A. Shyam, A. S. Aryan, C. S. A, R. H. A, V. Vipin, and A. Krishnan, "Design and analysis of small-scale horizontal axis wind turbine using PVC material," *Mater. Today Proc.*, vol. 52, pp. 2238–2254, 2021, doi: 10.1016/j.matpr.2021.08.095.

[11] D. Garcia-Ribeiro, J. A. Flores-Mezarina, P. D. Bravo-Mosquera, and H. D. Cer´on-Mu˜noz, "Parametric CFD analysis of the taper ratio effects of a winglet on the performance of a Horizontal Axis Wind Turbine," vol. 47, no. August, pp. 1–10, 2021, doi: 10.1016/j.seta.2021.101489.

[12] B. Navinkumar, K. M. Parammasivam, S. Rajendran, and V. Mohanavel, "CFD analysis of horizontal axis wind turbine braking system using chordwise spacing," *Mater. Today Proc.*, vol. 37, pp. 542–552, 2021, doi: 10.1016/j.matpr.2020.05.564.

[13] A. ArabGolarcheh, M. Anbarsooz, and E. Benini, "An Actuator Line Method for Performance Prediction of HAWTs at Urban Flow Conditions: A Case Study of Rooftop Wind Turbines," *Energy*, vol. 292, p. 130268, 2024, doi: 10.1016/j.energy.2024.130268.

[14] X. Du, J. Liang, G. Qian, Y. Yang, P. Xie, and K. Zhang, "A computational framework for the co-optimization of platform hydrodynamic and passive structural control of floating offshore wind turbines," *Ocean Eng.*, vol. 293, no. October 2023, pp. 1–17, 2024, doi: 10.1016/j.oceaneng.2023.116609.

[15] A. Khedr and F. Castellani, "Critical issues in the moving reference frame CFD simulation of small horizontal axis wind turbines," *Energy Convers. Manag. X*, vol. 22, no. February, pp. 1–19, 2024, doi: 10.1016/j.ecmx.2024.100551.

[16] J. Taghinezhad, S. Abdoli, V. Silva, S. Sheidaei, R. Alimardani, and E. Mahmoodi, "Computational fluid dynamic and response surface methodology coupling: A new method for optimization of the duct to be used in ducted wind turbines," *Heliyon*, vol. 9, no. 6, pp. 1–16, 2023, doi: 10.1016/j.heliyon.2023.e17057.

[17] Pratama Ricky Novianto, Fahrudin, D. Rhakasywi, and T. Juwairiyah, "Analysis of Blade Quantity Variations on Horizontal Axis Wind Turbine Type Taperless Airfoil SG6043 Using Blade Element Momentum (BEM)," *Tech. Rom. J. Appl. Sci. Technol.*, vol. 17, pp. 367–372, 2023, doi: 10.47577/technium.v17i.10109.

[18] K. Deghoum *et al.*, "An investigation of the Steady-State and Fatigue Problems of a Small Wind Turbine Blade

Based on the Interactive Design Approach Khalil," *Int. J. Renew. Energy Dev.*, vol. 657 LNNS, no. 1, pp. 396–406, 2023, doi: 10.1007/978-3-031-36201-9_34.
[19] S. Mauro, R. Lanzafame, M. Messina, and S. Brusca, "On the importance of the root-to-hub adapter effects on HAWT performance: A CFD-BEM numerical investigation," *Energy*, vol. 275, no. April, pp. 1–12, 2023, doi: 10.1016/j.energy.2023.127456.
[20] S. Rajamohan *et al.*, "Approaches in performance and structural analysis of wind turbines – A," *Sustain. Energy Technol. Assessments*, vol. 53, no. March, pp. 1–34, 2022, doi: 10.1016/j.seta.2022.102570.
[21] A. Li, G. R. Pirrung, M. Gaunaa, H. A. Madsen, and S. G. Horcas, "A computationally efficient engineering aerodynamic model for swept wind turbine blades," *Wind Energy Sci.*, vol. 7, no. 1, pp. 129–160, 2022, doi: 10.5194/wes-7-129-2022.
[22] S. Jain, N. Sitaram, and S. Krishnaswamy, "Effect of Reynolds Number on Aerodynamics of Airfoil with Gurney Flap," *Int. J. Rotating Mach.*, vol. 2015, no. 1, pp. 1–10, 2015, doi: 10.1155/2015/628632.
[23] D. Jha, M. Singh, and A. N. Thakur, "A novel computational approach for design and performance investigation of small wind turbine blade with extended BEM theory," *Int. J. Energy Environ. Eng.*, vol. 12, pp. 563–575, 2021, doi: https://doi.org/10.1007/s40095-021-00388-y.
[24] Z. Wang, C. Kang, Y. Zhang, H.-B. Kim, and and F. Jin, "Effect of blade chord length on startup performance of H-type tidal current turbine rotor," *AIP Adv.*, vol. 13, no. 3, pp. 1–12, 2023, doi: 10.1063/5.0141151.
[25] L. de L. Couto, N. E. Moreira, J. Y. de O. Saito, P. H. Hallak, and A. C. de C. Lemonge, "Multi-Objective Structural Optimization of a Composite Wind Turbine Blade Considering Natural Frequencies of Vibration and Global Stability," *Constraints*, vol. 16, no. 8, pp. 1–25, 2023, [Online]. Available: https://www.mdpi.com/1996-1073/16/8/3363.
[26] M. Grujicic, G. Arakere, E. Subramanian, V. Sellappan, A. Vallejo, and M. Ozen, "Structural-Response Analysis, Fatigue-Life Prediction, and Material Selection for 1 MW Horizontal-Axis Wind-Turbine Blades," *J. Mater. Eng. Perform.*, vol. 19, no. 6, pp. 790–801, 2010, doi: 10.1007/s11665-009-9558-8.